# Characteristics of agricultural phosphorus migration in different soil layers on purple soil sloping cropland under natural rainfall conditions

Yi Wang[1,2]*, Fangxin Chen[2], Huan Zhao[2,3], Deti Xie[2], Jiupai Ni[2]* and Dunxiu Liao[1]

[1]Chongqing Academy of Agricultural Sciences, Chongqing, China, [2]College of Resources and Environment, Southwest University, Chongqing, China, [3]Guizhou Academy of Agricultural Sciences, Guiyang, China

Limited by the current monitoring and collection methods of subsurface flow data, the characteristics of phosphorus (P) migration loss in different soil layers on sloping cropland under natural rainfall conditions need to be clarified. In this study, a reliable U-trough collection method was used to explore P migration losses in different purple soil layers ($L_0$: surface, $L_1$: 0−20 cm, $L_2$: 20−40 cm, and $L_3$: 40−60 cm) for purple soil sloping cropland during a field monitoring campaign spanning two calendar years under natural rainfall conditions. The results suggested that the annual surface P loss load was 1.08 kg*ha$^{-1}$*yr$^{-1}$, where 92.1% was particulate P. The annual leaching loss load of total P from the $L_1$ layer was 3.55 kg*ha$^{-1}$*yr$^{-1}$, where 74.2% and 10.5% were intercepted by the $L_2$ and $L_3$ layers, respectively, to increase the *in situ* soil P stocks. Only 15.3% of $L_1$'s annually leached P, and only half the surface P loss load ($L_0$), was lost to underground water. Heavy-rain events on the purple soils in the studied sloping cropland induced 43.9% of the annual surface P loss load. In contrast, 36.1%, 30.5%, and 30.3% of P's eventual annual leached loss loads resulted from heavy, moderate, and torrential rain events, respectively. The maize season was the main period of surface and subsurface P migration loss. Due to the limitation of experimental conditions, the results of this experiment could not represent the soil phosphorus migration process in the natural purple slope farmland in nature, but it could partially represent the soil phosphorus migration in the newly cultivated purple sloping cropland in Chongqing.

# 1 Introduction

Diffuse phosphorus (P) and nitrogen (N) loss from agricultural fields is the critical factor causing agricultural nonpoint source pollution (AGNSP), seriously damaging the ecological environment by water eutrophication and algal blooms (Bechmann et al., 2019; Cheng et al., 2021; Hanrahan et al., 2021). Soil P is derived from fertilizer and pesticide applications, soil parent material release, and atmospheric deposition, wherein fertilizer is the critical source of arable land soil P (Linderholm et al., 2012). Therefore, the regular location of P migration is

soil bodies, manifesting as temporary sinks or sources for P (Jahanzad et al., 2019; Weihrauch and Weber, 2021). Loss of P in farmland is an essential cause of eutrophication in the water environment, as P is transported from soils to rivers and other water bodies (He et al., 2019). Therefore, controlling the loss of P in soil is essential.

P migration is a complicated biogeochemical process that includes P accumulation, sorption–desorption, and water movement in the soil profile (Hua and Zhu, 2020). There are three major locations for fertilizer P: one is in planting roots for growth, approximately 30%, as some have reported (Wang, 2021), one is stored in the soil body to enrich the soil P storage by soil sorption and soil bacteria utilization, and the last is migrated from the *in situ* soil body by surface and subsurface runoff (Cameron et al., 2013). Particulate P (PP) loss is dominant in surface runoff and sediment (Bah et al., 2020), while dissolved reactive P (DRP) is the main form of P in subsurface runoff and soil leachate (Chen and Arai, 2020). McDowell et al. (2016) also noted that soil P loss is mainly caused by sediment transport in surface runoff. P mobilization in agricultural landscapes is affected by both hydrologic (transport) and biogeochemical (supply) processes interacting within soils (Plach et al., 2018), specifically embodied in erosion and runoff factors, which are the dominant pathways of agricultural nutrient loss ((Liu et al., 2012; Zhang et al., 2013). Factors affecting P migration are various and comprehensive (Wang et al., 2021a), among which surplus P input from fertilizers, especially chemical fertilizers, is the main factor increasing soil P losses (Fischer et al., 2018). Soil pores and fissures, especially macropores and cracks, provide migration channels for soil P.

Moreover, sloping farmland is one of the most serious agricultural P loss areas globally (Wang et al., 2018). Sixty percent of cultivated land in the Three Gorges Reservoir Area (TGRA), one of China's main economic development zones, is purple soil with rich porosity and high transitivity (Zhang et al., 2019; Wang et al., 2021b), which is convenient for soil nutrient migration. In 2016, the loss of chemical fertilizer in the TGRA reached $1.06 \times 104$ t, accounting for 8.9% of fertilizer consumption (MEP, 2020). Agricultural N and P losses have become major threats to water quality and agricultural development in the TRGA (Zhu et al., 2012; Zhang et al., 2015). Therefore, P losses in purple soil sloping farmland need greater attention (Luo et al., 2013).

In summary, previous studies have mainly focused on P loss in surface runoff, while research on the migration characteristics and loading from different soil layers is scarce and needs further study. Agricultural P mainly migrates from the top to the bottom soil layer in the soil body through soil pores under both gravity and water pressure; during the process, the migrated P fractions are intercepted and absorbed by soil particulates. However, the role of each soil layer is still unclear. Weihrauch and Weber (2021) suggested that the spatial hotspots of P loss are the top soils and the deep P stocks in the riparian buffer zones. Therefore, it is meaningful for the prevention and control of AGNSP to explore the P loss rule of each soil layer. In this paper, a reliable U-trough collection method (UCM) was used to analyze the agricultural P migration loss loads from different soil layers under natural rainfall. This study aimed to provide a practical reference for quantitative research on soil nutrient migration losses from different soil layers.

# 2 Materials and methods

## 2.1 Experimental site

The experimental site was located at the National Monitoring Base for Purple Soil Fertility and Fertilizer Efficiency, which is in Beibei District (29°48′38″N, 106°24′40.6″E), Chongqing Municipality, China (Figure 1A). This field is in the typical subtropical monsoon climate zone with a mean annual temperature of 18.3 °C and a mean annual precipitation of 1105.4 mm. The rainy season is mainly from May to October, overlapping with the hot season. This region is rich in low hilly landforms and sloping farmlands. The soil is mainly purple, classified as Pup-Orthic Entisols in Chinese Soil Taxonomy or Regosols in Food and Agricultural Organization (FAO) Taxonomy or Entisols in United States Department of Agriculture (USDA) Taxonomy. The soils are shallow (approximately 30 cm–80 cm depth), and the parent bedrock has poor water permeability. The soil for this study is developed from the Jurassic Shaximiao Formation. The basic physicochemical properties of each layer's soil are shown in Table 1. The common crop rotation in this region is summer maize rotated with winter mustard.

## 2.2 Experimental design

Each runoff field was constructed as a separate plot with dimensions of 9 m (length) × 3 m (width) × 0.8 m (depth). Each runoff plot's slope and soil depth were 15° and 60 cm, respectively. Adjacent ones were hydrologically isolated with cement walls to avoid unexpected interplot cross-flow between plots. A reinforced concrete floor was made to imitate the parent bedrock with poor water permeability. The test soil in each runoff field was filled in different soil layers ($L_1$: 0 cm–20 cm, $L_2$: 20 cm–40 cm, and $L_3$: 40 cm–60 cm) according to the technical code for the newly cultivated land in Chongqing. The open trench collected surface ($L_0$) flow and subsurface flow from three different soil layers were collected via U-shaped PVC conflux troughs settled on the bottom of each soil layer and conveyed to buckets by using water discharge tubes (Figure 1B). Each conflux trough (rectangle without cover, 10 cm width, 5 cm depth) was of the same length, parallel to the experimental field, and then, filled with clean quartz sand and covered by two layers of 200-mesh gauze to enhance the trough's hydraulic conductivity (Wang et al., 2021a). Runoff with sediment samples could be obtained in each corresponding bucket. The possible overflow was collected into a sub-bucket by using a pipe (nominal diameter 32 mm) to measure the overflow from the bucket to obtain the accurate runoff flow of each plot. Specifically, to improve the test accuracy, two identical collection troughs for each soil layer of a single runoff plot and three runoff plots with the same treatment (as three replicates) were conducted. Conventional along-slope cropping and fertilization were conducted according to farmers' planting habits. The fertilization amounts and dates for different crops during the test period (**3/1/2018-2/29/2020**) are shown in Table 2.
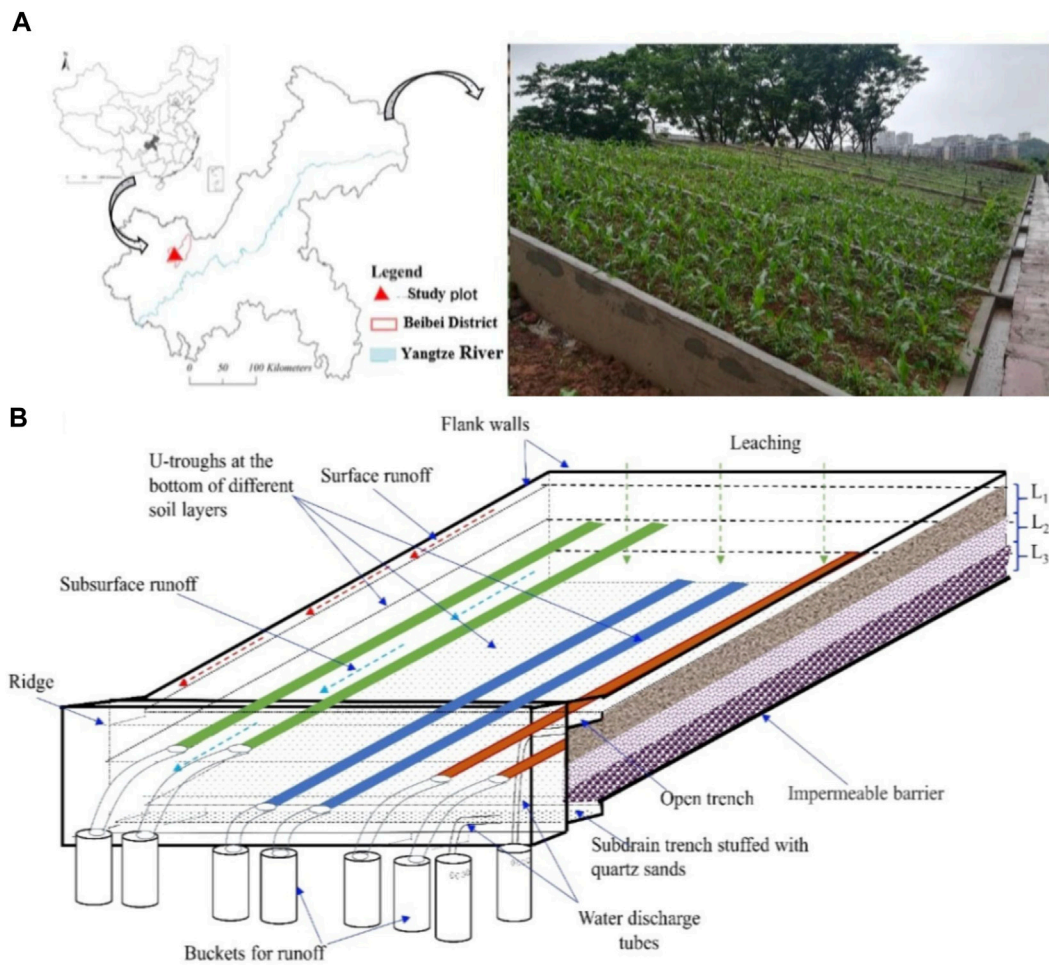
**FIGURE 1**
Location of test plots **(A)** and layout of the U-trough collection method (UCM) **(B)**. $L_1$: 0 cm–20 cm, $L_2$: 20 cm–40 cm, and $L_3$: 40 cm–60 cm.

**TABLE 1 Basic properties of experimental soil.**

| Soil layer | pH | STN (g/kg) | SAN (mg/kg) | STP (g/kg) | SAP (mg/kg) | STK (g/kg) | SRAK (mg/kg) | SOM (g/kg) | SBD (g/cm³) | SP (%) | ST |
|---|---|---|---|---|---|---|---|---|---|---|---|
| $L_1$ (0–20 cm) | 6.29 | 1.14 | 103.66 | 0.72 | 57.71 | 21.65 | 88.43 | 14.96 | 1.22 | 53.96 | Sandy clay |
| $L_2$ (20–40 cm) | 7.34 | 1.11 | 93.08 | 0.74 | 45.94 | 21.86 | 87.71 | 14.91 | 1.32 | 50.19 | |
| $L_3$ (40–60 cm) | 8.15 | 0.76 | 33.45 | 0.64 | 36.9 | 20.35 | 43.65 | 0.67 | 1.46 | 46.45 | |

STN, soil total nitrogen; SAN, soil available nitrogen; STP, soil total phosphorus; SAP, soil available phosphorus; STK, soil total potassium; SRAK, soil rapidly available potassium; SOM, soil organic matter; SBD, soil bulk density; SP, soil porosity; ST, soil texture.

**TABLE 2 Fertilizer application per unit cropland area during the test period (pure amount).**

| Crop | N (kg/ha) | $P_2O_5$ (kg/ha) | $K_2O$ (kg/ha) | Fertilizing date |
|---|---|---|---|---|
| Maize (seedling fertilizer) | 110 | 40 | 50 | 2018/4/1; 2019/4/4 |
| Maize (additional fertilizer) | 220 | 80 | 100 | 2018/5/15; 2019/5/19 |
| Mustard | 510 | 255 | 285 | 2018/11/21; 2019/11/15 |

N, $P_2O_5$, and $K_2O$ are the abbreviations of nitrogen, phosphorus pentoxide, and potassium oxide.

## 2.3 Sampling and measuring

The observation of P migration from different soil layers by runoff and sediment was **from March 2018 to February 2020**. Hourly meteorological data were obtained from a small automatic-collection weather station near the research plots. Soil samples were taken with auger and ring samples before planting and after harvesting. The basic physicochemical properties of the soil and sediment samples were determined by following Yang et al.'s (2008) methods.

After each rainfall-runoff event, the volumes of surface flow and subsurface flow from each soil layer in each runoff plot were monitored. Subsequently, water samples of surface and subsurface flow in the buckets were collected separately and then analyzed promptly in the laboratory. Water samples from surface and subsurface flows were used to measure sediment yield after oven drying at 105 °C for 24 h and the concentrations of P fractions. The total phosphorus (TP) concentration in the water samples was measured without filtration. Water samples used to analyze the phosphate–phosphorus ($PO_4^{3-}$–P) concentration and total dissolved phosphorus (TDP) were filtered through 0.45 μm filtration membranes. After digestion with potassium persulfate, TP and TDP concentrations were determined through the molybdenum blue colorimetry method (Huang et al., 2020). The concentration of $PO_4^{3-}$–P was measured using the same method used for TDP without digestion. The PP concentration was calculated by the following equation: PP = TP−TDP (Li et al., 2017). The TP content of each soil layer was determined by the molybdenum blue colorimetry method after melting with NaOH, while the available phosphorus (AP) was measured by the Olsen method (Wang, 2021). The sediment samples were dried in an oven at 105 °C to a constant weight. The conventional pipette method determined the sediment particle size distribution (PSD) (Zuo et al., 2020).

## 2.4 Experimental data collection and processing

Each fluid sample's runoff volume was the water collected in the corresponding bucket of each collection device. The runoff flux of surface runoff and subsurface runoff under the $i$th rainfall event was calculated by the following formulas, modified from the work of Peng et al. (2016):

$$R_{sur\,i} = \frac{r_{sur\,i}}{A * COS(15°)}, \tag{1}$$

$$R_{ni} = \frac{r_{ni}}{a * COS(15°)}, \tag{2}$$

$$\Delta R_{ni} = R_{n-1\,i} - R_{ni}, \tag{3}$$

where $R_{sur\,i}$ is the surface runoff flux under the $i$th rainfall event (mm); $r_{sur\,i}$ is the collected surface runoff volume (L); A is the area of a single test plot (m²); 15° is the slope of the test plot; $R_{ni}$ is the subsurface runoff flux at the $n$th soil layer (mm); $r_{ni}$ is the collected subsurface runoff volume at the $n$th soil layer (L); n is the number of soil layers (L₁: 0 cm–20 cm depth; L₂: 20 cm–40 cm depth; and L₃: 40 cm–60 cm depth); a is the area of a single collection device (m²); and $\Delta R_{n-1\,i}$ is the retention amount of subsurface runoff at the layer of $n$-1 (mm). When n = 1, $R_{0\,i}$ is the whole permeation flux of rainfall

through the soil surface, which is approximately equal to the gap of precipitation and surface runoff; when n = 4, $R_{4i}$ is the final subsurface runoff flux lost from the whole soil layers.

The following formulas were used to calculate the P migration load of the surface and subsurface under the $i$th rainfall event:

$$Q_{sur\,ij} = \frac{r_{sur\,i} * C_{sur\,ij}}{A * COS(15°)} * 10^4 / 10^3, \tag{4}$$

$$Q_{nij} = (\frac{r_{ni} * C_{nij}}{a * COS(15°)} * 10^4 / 10^3, \tag{5}$$

$$\Delta Q_{nij} = Q_{n-1\,ij} - Q_{nij}, \tag{6}$$

where $Q_{sur\,ij}$ is the $j$th nutrient migration load in surface runoff under the $i$th rainfall event (g/ha); $C_{sur\,ij}$ is the concentration of the $j$th nutrient in surface runoff (mg/L); $Q_{nij}$ is the $j$th nutrient migration load (g/ha); $C_{nij}$ is the concentration of the $j$th nutrient at the $n$th soil layer (mg/L); and $\Delta Q_{nij}$ is the retention load of the $j$th nutrient at layer $n$-1 (g/ha). When $\Delta Q_{nij}$ is positive, it indicates that this layer intercepts N under the rainfall event; otherwise, it plays a releasing role in P migration. When n = 1, $Q_{0ij}$ represents the overall leaching amount of the $j$th nutrient through the soil surface, approximately equal to the $j$th nutrient gap in rainfall and surface runoff. When n = 4, $\Delta R_{3i}$ is the $j$th nutrient final loss load through subsurface runoff from the whole soil layer.

This study analyzed the migration loads of P under different planting stages (S₁: maize season, S₂: summer fallow period, S₃: mustard season, and S₄: winter fallow period) and different rainfall patterns (*TR*: torrential rain, *HR*: heavy rain, *MR*: moderate rain, and *LR*: light rain, classified by the Classification Standard of China Meteorological Administration), as shown in Figure 2.

## 2.5 Statistical analysis

IBM SPSS Statistics 26 was the data analysis tool utilized in this study, and GraphPad Prism 8 was the mapping software used in this paper. Pearson correlation was used for the correlation analysis. The least significant difference (LSD) method at $p$ = 0.05 was performed to elucidate any significant differences between different levels.

# 3 Results

## 3.1 Rainfall-runoff characteristics

There were differences in the annual cumulative rainfall and each soil layer's annual cumulative runoff loss between different rainfall patterns in the test period. Figure 3A shows that the annual cumulative rainfall amounts of TR, HR, MR, and LR were 137.9, 246.1, 338.9, and 286.3 mm, accounting for 13.7%, 24.4%, 33.6%, and 28.4% of the annual cumulative rainfall, respectively. However, the differences in annual cumulative rainfall amounts between different rainfall patterns were nonsignificant. Figure 3B suggests that, except for the annual loss of surface runoff, the annual cumulative subsurface runoff loss amount measured from each soil layer decreased with increasing soil depth. The annual surface runoff losses under TR, HR, MR, and LR were 19.4, 26.0, 22.3, and 2.5 mm, respectively. The corresponding rainfall-surface runoff rates were 14.1%, 10.6%, 6.6%, and 0.9%, respectively,
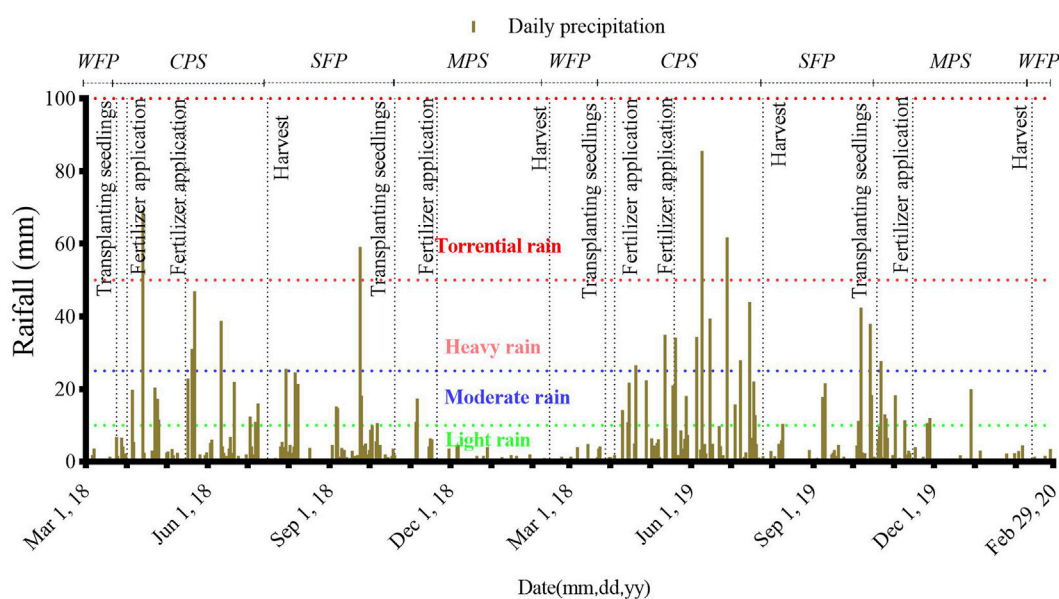
**FIGURE 2**
Temporal distribution of natural daily rainfall in the experimental plot during the testing period. *WFP*: winter fallow period; *CPS*: maize planting stage; *SFP*: summer fallow period; and *MPS*: mustard planting stage.

indicating that the lower the rainfall grade was, the more difficult it was to produce surface runoff. The annual cumulative amounts of intercepted subsurface flow were 63.2 mm (TR), 144.4 mm (HR), 220.6 mm (MR), and 270.1 mm (LR), accounting for 45.8%, 58.7%, 65.1%, and 94.3% of the annual cumulative rainfall, respectively. The lower the rainfall grade was, the higher the proportion of the intercepted flow of supplying soil water to the total rainfall. The subsurface runoff loss amounts from the $L_1$ layer under different rainfall patterns were 102.7 mm (TR), 166.7 mm (HR), 165.1 mm (MR), and 28.4 mm (LR), which meant that the intercepted amounts of the $L_1$ layer were 25.0%, 37.0%, 68.7%, and 94.6% of the total intercepted amounts under different rainfall patterns, respectively. The subsurface flow flux decreased significantly with increasing soil depth. In contrast, the intercepted subsurface runoff decreased, which meant that the interception ability of the soil layer for permeated subsurface runoff weakened with increasing soil depth. The eventual annual loss amounts of subsurface runoff under various rainfall patterns were only 46.7% (TR), 34.4% (HR), 30.3% (MR), and 4.8% (LR) of the annual total amounts permeated into the soil and only 40.1% (TR), 30.8% (HR), 28.4% (MR), and 4.8% (LR) of the annual cumulative rainfall.

The distributions of the rainfall and runoff loss amounts of each planting stage were uneven during the whole test period. Figure 3C shows that 56.0% and 29.1% of the annual rainfall amounts were from the maize season ($S_1$: 571.3 mm) and summer fallow period ($S_2$: 281.5 mm), respectively; only 12.9% and 2.0% were from the mustard season ($S_3$) and winter fallow period ($S_4$), respectively. Figure 3D shows that 67.7% of the annual surface runoff loss amount and 79.1% of the annual subsurface loss amount occurred in the maize season; 25.9% of the annual surface runoff loss amount and 12.0% of the annual subsurface loss amount occurred in the summer fallow period. No surface or subsurface runoff loss phenomenon was found due to the slightly scattered rainfall in the winter fallow

period. The annual surface runoff loss and each soil layer's annual subsurface runoff loss amount decreased from $S_1$ to $S_4$ seasons. The annual subsurface runoff-permeated loss amount in each planting season significantly decreased with the increase in soil depth ($p < 0.05$).

## 3.2 Phosphorus migration loss characteristics under different rainfall patterns

The difference between the average migration loss intensities of P per rainfall-runoff event under different rainfall patterns was significant. As shown in Figure 4, each soil layer's average P migration loss intensity per rainfall-runoff event increased remarkably with increasing rainfall grades. Notably, the average surface migration loss intensities of TP and PP measured under the TR pattern were exceptionally higher than those measured under other rainfall patterns. The average leached loss intensities of each form's P decreased sharply from soil depths of 20 cm–40 cm under each rainfall pattern. The average leached loss intensities of TP and PP at the 40 cm depth were significantly lower than those at the 20 cm depth, indicating that the 20 cm–40 cm soil layer intercepted most of the leached TP and PP from the 0 cm–20 cm soil layer under all rainfall events. The rainfall patterns significantly affected the average migration loss intensities of TP and PP in the surface runoff. The change characteristics of the average migration loss intensities of TDP and $PO_4^{3-}$–P per rainfall-runoff event under each rainfall pattern showed the same trends. In summary, the higher the rainfall intensity was, the greater the TP and PP migrating loads through runoff were.

**FIGURE 3**
Annual cumulative rainfall **(A)** and runoff permeating loss from different soil layers **(B)** under different rainfall grade, and annual cumulative rainfall **(C)** and runoff permeating loss from different soil layers **(D)** under different planting stages. $L_1$, $L_2$, and $L_3$ represent the soil layer of 0 cm––20 cm, 20 cm–40 cm, and 40 cm–60 cm under the soil surface, respectively. Values of L0 represent the loss of surface runoff, and values of L1, L2, and L3 represent the loss of subsurface runoff. *TR, HR, MR, and LR are the abbreviations of* torrential rain, heavy rain, moderate rain, and light rain, respectively. $S_1$, $S_2$, $S_3$, and $S_4$ represent the maize, summer fallow, mustard, and winter fallow period, respectively. The capital letters represent the significant difference between different rainfall grades or planting stages at $p = 0.05$; the lowercase letters represent the significant difference between different soil layers at $p = 0.05$.
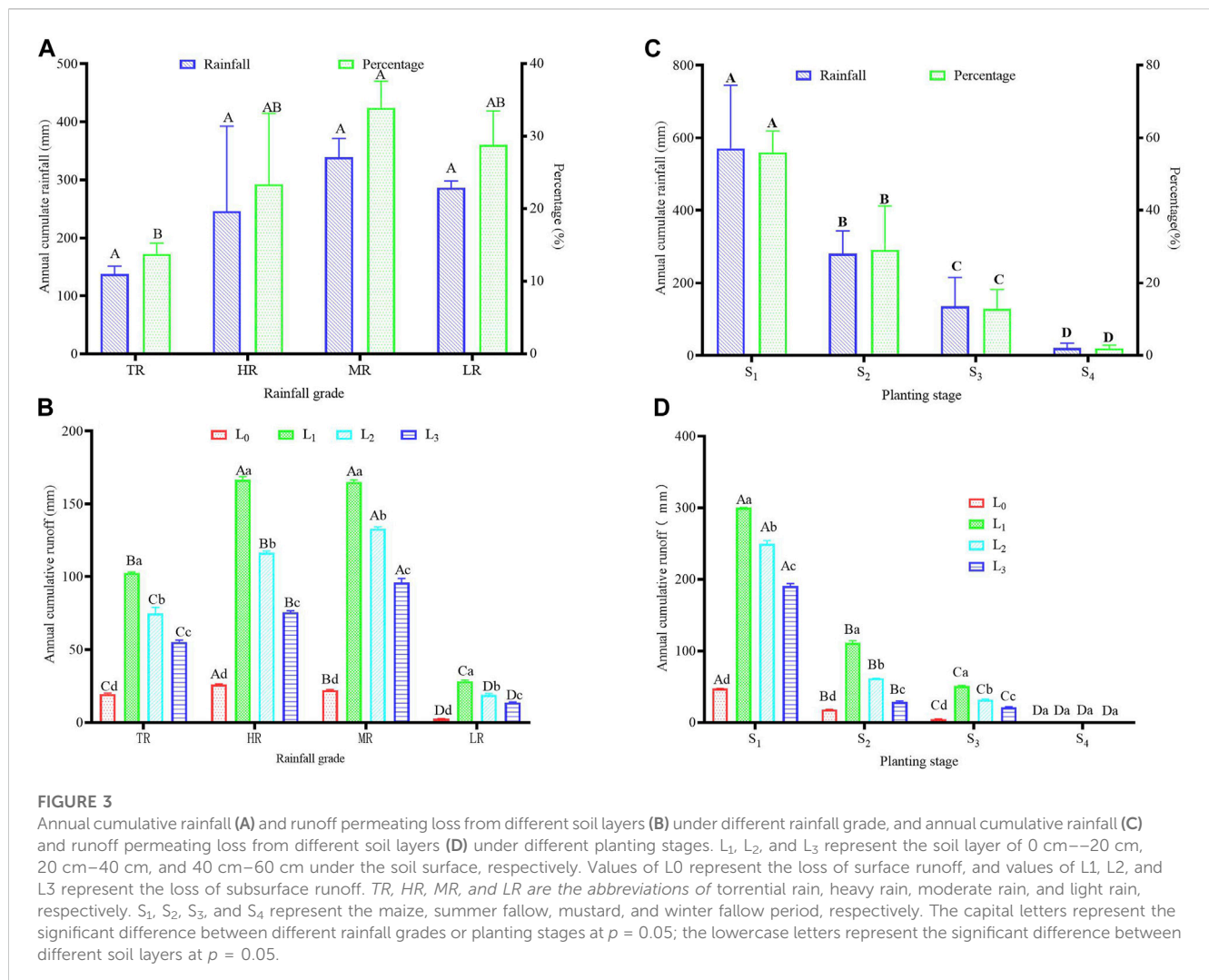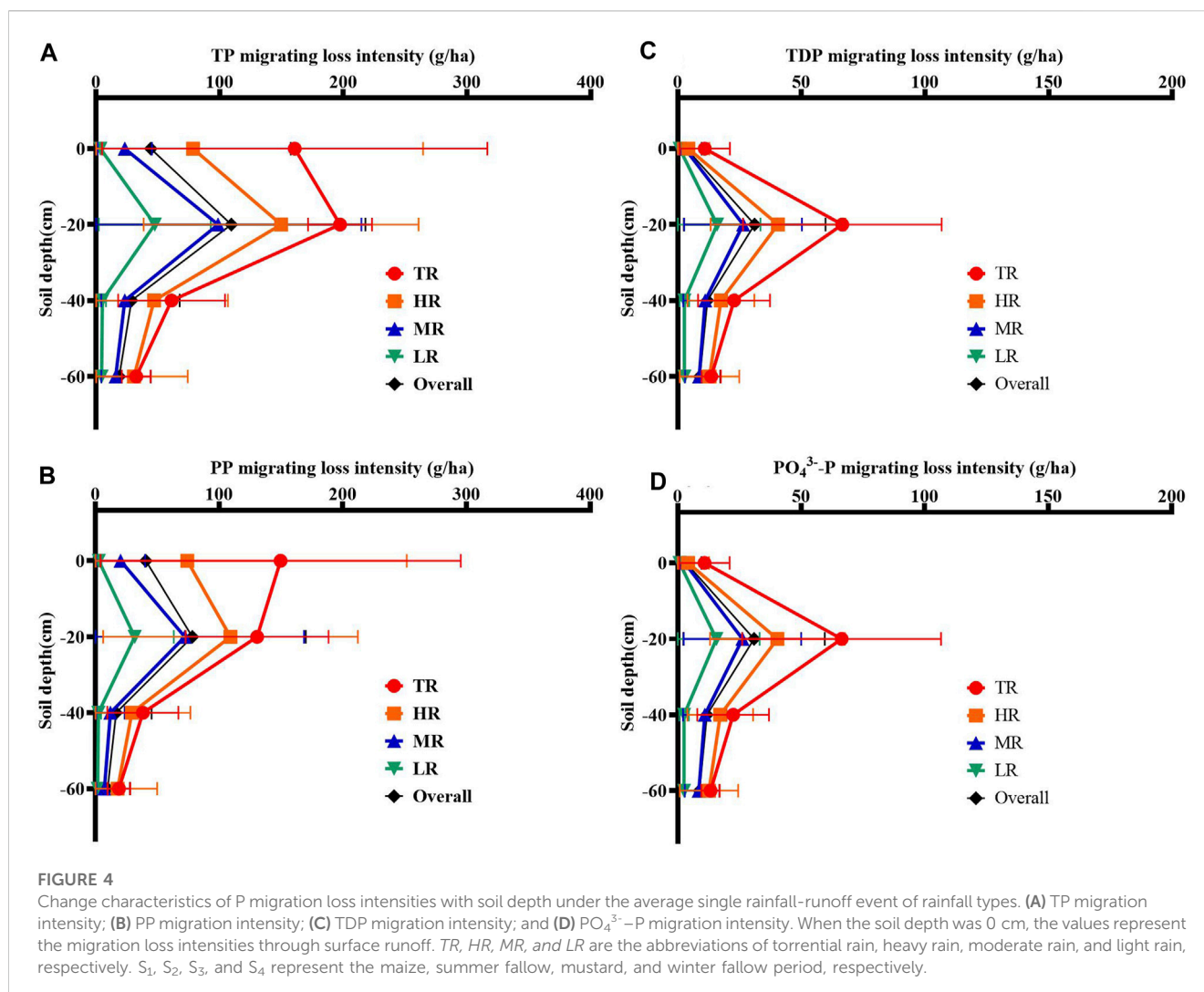
Figure 5 shows that each form of P's leached loss intensities from each soil layer presented positive linear relationships with rainfall. The leached loss intensities of each form of P from each soil layer increased significantly with rainfall. The regression coefficient between each soil layer's leached loss intensities of various P and rainfall decreased with increasing soil depth, which meant that the effect of rain on each leached P loss intensity decreased with the increase in soil depth. Notably, the gaps of each form's P leached loss intensities between the $L_1$ layer and $L_2$ layer were significantly higher than those between the $L_2$ layer and $L_3$ layer, indicating that the interception ability of the $L_2$ layer was significantly higher than that of the $L_3$ layer.

As shown in Table 3, the average annual migration loss loads of each form's P from different soil layers under different rainfall patterns were significantly different. The TR, HR, MR, and LR patterns caused 1041.09 g*ha$^{-1}$*yr$^{-1}$, 1884.35 g*ha$^{-1}$*yr$^{-1}$, 1551.64 g*ha$^{-1}$*yr$^{-1}$, and 153.99 g*ha$^{-1}$*yr$^{-1}$ of TP yearly migration loss from the $L_1$ layer, 29.0% (302.27 mm), 25.2% (474.67 mm), 18.4% (285.11 mm), and 12.3% (18.95 mm) of which was lost through surface runoff, respectively. It was concluded that the higher the rainfall grade was, the higher the proportion of the annual surface loss to the $L_1$ layer's total annual migration loss was. Additionally, 71.9% of the TP's annual surface loss occurred under the TR and HR patterns.

The annual leached loss loads of TP from $L_1$ and $L_2$ under TR, HR, MR, and LR were 738.82 g*ha$^{-1}$*yr$^{-1}$, 1409.68 g*ha$^{-1}$*yr$^{-1}$, 1266.53 g*ha$^{-1}$*yr$^{-1}$, and 135.04 g*ha$^{-1}$*yr$^{-1}$ and 259.05 g*ha$^{-1}$*yr$^{-1}$, 295.52 g*ha$^{-1}$*yr$^{-1}$, 332.70 g*ha$^{-1}$*yr$^{-1}$, and 30.15 g*ha$^{-1}$*yr$^{-1}$, respectively, indicating that the $L_2$ layer intercepted 64.9%, 79.0%, 73.7%, and 77.7% of the $L_1$ layer's leached TP. The annual leached loss loads of TP from the $L_3$ layer under the TR, HR, MR, and LR grades were 163.96 g*ha$^{-1}$*yr$^{-1}$, 195.53 g*ha$^{-1}$*yr$^{-1}$, 165.07 g*ha$^{-1}$*yr$^{-1}$, and 17.36 g*ha$^{-1}$*yr$^{-1}$, respectively, indicating that the $L_3$ layer intercepted 12.9%, 7.1%, 13.2%, and 9.5% of the $L_1$ layer's leached TP, respectively.

The annual surface migration loss loads of PP under different rainfall patterns were 91.8% (TR), 94.6% (HR), 88.7% (MR), and 83.6% (LR) of the surface migration loss loads of TP. The annual leached loss loads of PP underground under different rainfall patterns were 70.4% (TR), 83.4% (HR), 74.1% (MR), and 58.2% (LR) of the annual leached loss loads of TP underground. According to one-way ANOVA, except for TDP, the annual migration loss loads of each form's P under different rainfall grades showed significant differences. The annual surface migration loss loads of each form's P and the annual leached loss loads of each form's P at each soil layer under the TR, HR, and MR grades were significantly higher than those under LR. Notably, TR and HR were the major

**FIGURE 4**
Change characteristics of P migration loss intensities with soil depth under the average single rainfall-runoff event of rainfall types. **(A)** TP migration intensity; **(B)** PP migration intensity; **(C)** TDP migration intensity; and **(D)** $PO_4^{3-}-P$ migration intensity. When the soil depth was 0 cm, the values represent the migration loss intensities through surface runoff. *TR, HR, MR, and LR* are the abbreviations of torrential rain, heavy rain, moderate rain, and light rain, respectively. $S_1$, $S_2$, $S_3$, and $S_4$ represent the maize, summer fallow, mustard, and winter fallow period, respectively.

rainfall patterns that caused P surface migration losses; however, HR and MR were the primary rainfall grades that induced underground leached P losses.

## 3.3 Phosphorus migration loss characteristics in different planting stages

The annual migration loss loads of different P forms from the same soil layer in different planting stages were significantly different. The annual migration loss loads of each form's P in different planting stages mostly occurred in the $S_1$ and $S_2$ stages. There was no observed migration loss of each form's P from every soil layer in the $S_4$ stage. Table 4 shows that the annual migration loss loads of surface TP in different planting stages were 850.03 g*ha$^{-1}$*yr$^{-1}$ ($S_1$), 193.39 g*ha$^{-1}$*yr$^{-1}$ ($S_2$), 37.58 g*ha$^{-1}$*yr$^{-1}$ ($S_3$), and 0.00 g*ha$^{-1}$*yr$^{-1}$ ($S_4$), accounting for 78.6%, 17.9%, 3.5%, and 0.0% of the annual total surface migration loss load of TP, respectively. There was no observed migration loss of each form's P from every soil layer in the $S_4$ stage. The annual leached loss loads of TP from different soil layers were 3550.07 g*ha$^{-1}$*yr$^{-1}$ ($L_1$), 917.43 g*ha$^{-1}$*yr$^{-1}$ ($L_2$), and 541.91 g*ha$^{-1}$*yr$^{-1}$ ($L_3$). The sequence of the

contribution rates of each soil layer's TP leached loss loads in different planting stages to the corresponding soil layer's annual total leached loss loads were 60.7% ($S_1$), 31.9% ($S_2$), 7.4% ($S_3$), and 0.0% ($S_4$) at the $L_1$ layer, 62.8% ($S_1$), 30.1% ($S_2$), 7.1% ($S_3$), and 0.0% ($S_4$) at the $L_2$ layer, and 73.0% ($S_1$), 14.7% ($S_2$), 12.3% ($S_3$), and 0.0% ($S_4$) at the $L_3$ layer. Except for the $S_4$ stage, the percentage of PP surface loss loads to the TP surface loss load in each planting stage gradually decreased from 93.0% ($S_1$) to 83.3% ($S_3$), while the percentages of the leached PP loss load to the leached TP loss load in each planting stage were 75.0% ($S_1$), 79.4% ($S_2$), and 76.0% ($S_3$). The percentages of the leached $PO_4^{3-}$-P loss load to the leached TP loss load in each planting stage gradually increased from 5.4% ($S_1$) to 14.7% ($S_3$).

## 3.4 Annual total migration loss loads from different soil layers

Figure 6 shows that soil layers significantly differed in each form of P's annual migration loss loads. The annual surface loss loads of different forms of P were 1.08 kg*ha$^{-1}$*yr$^{-1}$ (TP), 0.99 kg*ha$^{-1}$*yr$^{-1}$ (PP), 0.09 kg*ha$^{-1}$*yr$^{-1}$ (TDP), and 0.07 kg*ha$^{-1}$*yr$^{-1}$ ($PO_4^{3-}$-P). The
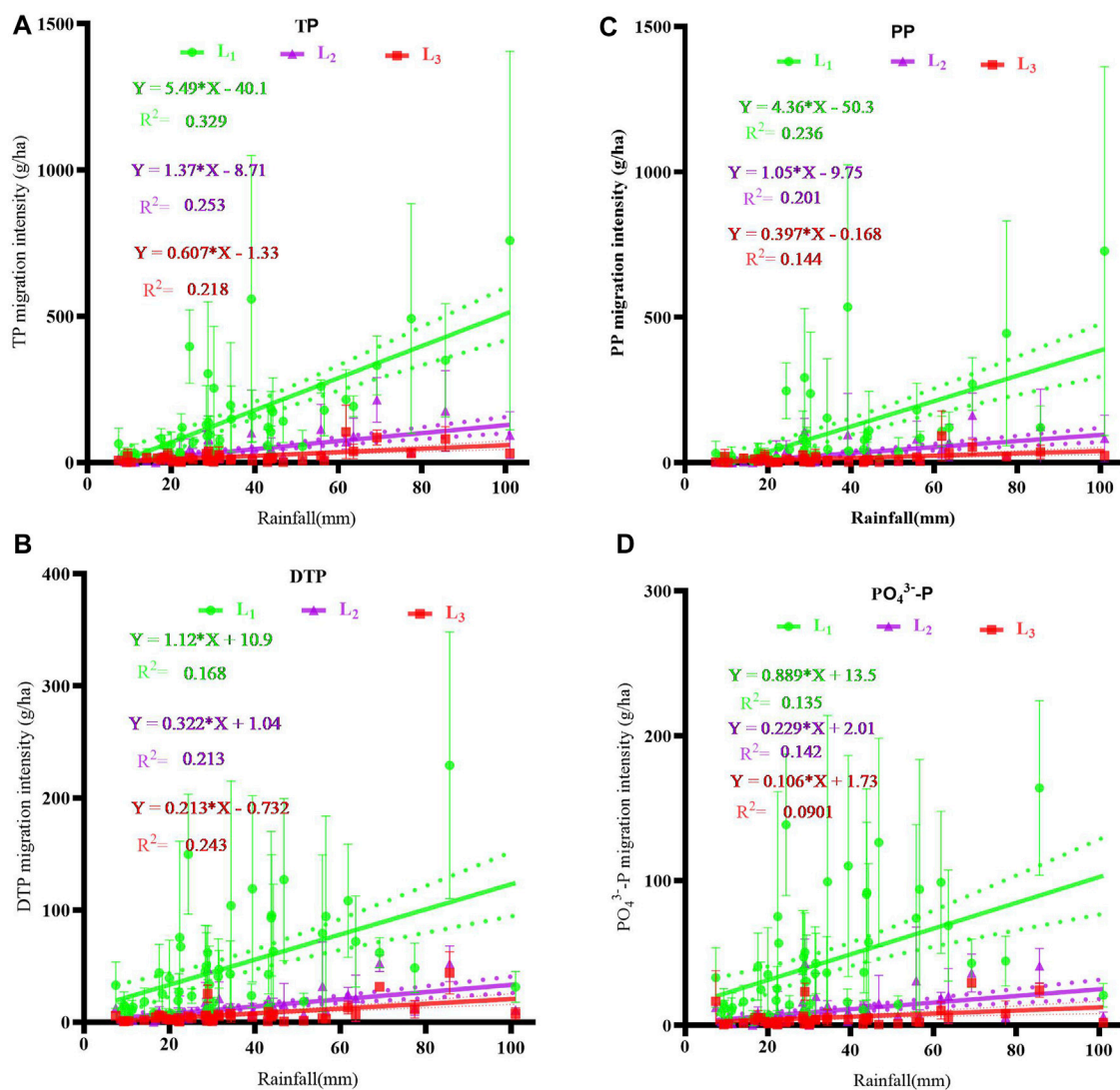
**FIGURE 5**
Correlation between migration intensities of each soil layer's different P forms and rainfall. **(A)** TP, **(B)** TDP, **(C)** PP, and **(D)** $PO_4^{3-}$–P. $L_1$, $L_2$, and $L_3$ represent the soil layers of 0 cm–20 cm, 20 cm–40 cm, and 40 cm–60 cm under the cultivated land surface, respectively. Values of L1, L2, and L3 in this figure represent the loss intensities of P through subsurface runoff, respectively. TP, DTP, PP, and $PO_4^{3-}$–P are the abbreviations of total phosphorus, total dissolved phosphorus, particulate phosphorus, and phosphate–phosphorus, respectively. The solid line is the best-fitting line for simple linear regression analysis, and the dotted line is the 95% confidence band.

eventual annual leached loss load of each form's P was 0.54 kg*ha$^{-1}$*yr$^{-1}$ (TP), 0.41 kg*ha$^{-1}$*yr$^{-1}$ (PP), 0.13 kg*ha$^{-1}$*yr$^{-1}$ (TDP), and 0.10 kg*ha$^{-1}$*yr$^{-1}$ ($PO_4^{3-}$–P), accounting for 50.1%, 41.3%, 152.3%, and 151.5% of their annual total surface migration loss loads, respectively. TP's annual leached loss load from the $L_1$ layer was up to 3.55 kg*ha$^{-1}$*yr$^{-1}$, among which 65.2% was PP. TP's annual leached loss loads from the $L_2$ and $L_3$ layers were 0.92 kg*ha$^{-1}$*yr$^{-1}$ and 0.54 kg*ha$^{-1}$*yr$^{-1}$, among which 68.2% and 75.8% were PP, respectively. The surface loss loads of PP and $PO_4^{3-}$–P accounted for 92.0% and 6.3% of the annual total surface TP loss load, respectively, while the underground eventual leached loss loads were 75.8% and 19.0% of the annual total underground leached loss load of TP, respectively. According to one-way ANOVA and the LSD test, the annual leached loss loads of TP and PP weakened significantly with the increase in soil depth ($p < 0.05$).

# 4 Discussion

Surface and underground leaching losses were the two major routes by which P was lost on the studied purple soil sloping cropland under natural rainfall conditions. Most studies have reported that soil P losses are mainly caused by surface sediment transport (McDowell et al., 2016; Deng et al., 2020; Pisani et al., 2020). However, in this study, it was found that the cultivated soil layer's annual leaching P loss load was approximately three times the annual surface P loss load. P's eventual annual leaching loss load from the bottom of the parent material layer was only half of the annual surface loss loads. In this study, P loss mainly consisted of PP losses through surface runoff; this result was consistent with the research results of McDowell et al. (2016). In this study, the proportion of surface PP loss load to the total surface P loss

**TABLE 3 Annual migration loss loads of different P forms from each soil layer under different rainfall patterns.**

| P form | Rainfall grade | $L_0$ (g*ha$^{-1}$*yr$^{-1}$) | | $L_1$ (g*ha$^{-1}$*yr$^{-1}$) | | $L_2$ (g*ha$^{-1}$*yr$^{-1}$) | | $L_3$ (g*ha$^{-1}$*yr$^{-1}$) | |
|---|---|---|---|---|---|---|---|---|---|
| | | Mean | SD | Mean | SD | Mean | SD | Mean | SD |
| TP | TR | 302.27a | 38.40 | 738.82c | 131.56 | 259.05b | 30.40 | 163.96b | 1.75 |
| | HR | 474.67a | 93.23 | 1409.68a | 135.80 | 295.52ab | 12.83 | 195.53a | 3.82 |
| | MR | 285.11a | 2.62 | 1266.53b | 116.66 | 332.70a | 3.25 | 165.07b | 0.49 |
| | LR | 18.95b | 0.77 | 135.04d | 7.58 | 30.15c | 3.62 | 17.36c | 1.86 |
| TDP | TR | 24.64a | 2.08 | 243.68a | 59.37 | 74.00a | 9.77 | 48.57a | 3.99 |
| | HR | 25.67a | 0.49 | 453.66a | 100.12 | 84.60a | 10.71 | 32.53a | 4.20 |
| | MR | 32.24a | 0.05 | 467.22a | 14.71 | 117.79a | 23.57 | 42.70a | 6.10 |
| | LR | 3.10a | 0.80 | 72.29a | 7.14 | 15.61a | 4.29 | 7.27a | 1.47 |
| PP | TR | 277.63ab | 36.32 | 495.14ab | 72.19 | 185.05a | 20.63 | 115.38b | 2.25 |
| | HR | 449.00a | 92.74 | 956.03a | 235.93 | 210.92a | 23.53 | 163.00a | 0.38 |
| | MR | 252.87b | 2.57 | 799.31a | 101.96 | 214.92a | 26.82 | 122.37b | 5.62 |
| | LR | 15.85c | 0.03 | 62.75b | 0.44 | 14.54b | 7.91 | 10.10c | 3.33 |
| PO$_4^{3-}$–P | TR | 20.50b | 0.61 | 211.01ab | 58.25 | 51.38bc | 2.01 | 36.26a | 0.77 |
| | HR | 14.98c | 2.10 | 419.11a | 95.57 | 69.61ab | 12.54 | 21.65b | 0.77 |
| | MR | 29.41a | 0.22 | 424.97a | 17.18 | 101.79a | 21.70 | 37.74a | 1.31 |
| | LR | 3.03d | 0.84 | 67.95b | 9.17 | 14.58c | 4.30 | 7.12c | 1.41 |

TR, HR, MR, and LR, are the abbreviations of torrential, heavy, moderate, and light rain, respectively. TP, DTP, PP, and PO$_4^{3-}$–P are the abbreviations of total phosphorus, total dissolved phosphorus, particulate phosphorus, and phosphate–phosphorus, respectively. L0 represents the cultivated land surface. $L_1$, $L_2$, and $L_3$ represent the soil layers of 0 cm–20 cm, 20 cm–40 cm, and 40 cm–60 cm under the cultivated land surface, respectively. The lowercase letters represent the significant difference in each soil layer's nutrient annual migration loss loads between rainfall patterns at $p$ = 0.05. SD represents standard deviation.

**TABLE 4 Annual migration loss loads of different P forms from each soil layer under different planting stages.**

| P form | Planting stage | $L_0$ (g*ha$^{-1}$*yr$^{-1}$) | | $L_1$ (g*ha$^{-1}$*yr$^{-1}$) | | $L_2$ (g*ha$^{-1}$*yr$^{-1}$) | | $L_3$ (g*ha$^{-1}$*yr$^{-1}$) | |
|---|---|---|---|---|---|---|---|---|---|
| | | Mean | SD | Mean | SD | Mean | SD | Mean | SD |
| TP | $S_1$ | 850.03a | 66.32 | 2153.49a | 190.77 | 576.14a | 50.36 | 395.60a | 8.32 |
| | $S_2$ | 193.39b | 6.40 | 1132.78b | 68.61 | 275.79b | 25.20 | 79.83b | 1.52 |
| | $S_3$ | 37.58c | 3.23 | 263.80c | 2.17 | 65.50c | 14.46 | 66.48b | 2.90 |
| | $S_4$ | 0.00c | 0.00 | 0.00c | 0.00 | 0.00c | 0.00 | 0.00c | 0.00 |
| TDP | $S_1$ | 59.70a | 0.18 | 906.18a | 108.52 | 213.62a | 54.04 | 98.72a | 3.81 |
| | $S_2$ | 19.67b | 1.53 | 202.96b | 58.81 | 45.76b | 6.77 | 16.41b | 3.20 |
| | $S_3$ | 6.28c | 0.63 | 127.71b | 14.00 | 32.62b | 1.06 | 15.94b | 0.02 |
| | $S_4$ | 0.00d | 0.00 | 0.00b | 0.00 | 0.00b | 0.00 | 0.00c | 0.00 |
| PP | $S_1$ | 790.33a | 66.51 | 1247.31a | 82.25 | 362.52a | 3.68 | 296.88a | 4.51 |
| | $S_2$ | 173.72b | 4.88 | 929.82b | 127.42 | 230.03b | 18.43 | 63.43b | 4.73 |
| | $S_3$ | 31.30c | 2.60 | 136.09c | 16.17 | 32.89c | 15.52 | 50.54b | 2.92 |
| | $S_4$ | 0.00c | 0.00 | 0.00c | 0.00 | 0.00c | 0.00 | 0.00c | 0.00 |
| PO$_4^{3-}$–P | $S_1$ | 46.15a | 1.35 | 824.08a | 111.68 | 175.47a | 44.29 | 83.05a | 1.80 |
| | $S_2$ | 16.25b | 0.93 | 185.60b | 52.59 | 36.60b | 6.58 | 10.31b | 1.15 |
| | $S_3$ | 5.52c | 1.04 | 113.35b | 15.90 | 25.28b | 2.84 | 9.41b | 0.22 |
| | $S_4$ | 0.00d | 0.00 | 0.00b | 0.00 | 0.00b | 0.00 | 0.00c | 0.00 |

TP, DTP, PP, and PO$_4^{3-}$–P are the abbreviations of total phosphorus, total dissolved phosphorus, particulate phosphorus, and phosphate–phosphorus, respectively. L0 represents the cultivated land surface. $L_1$, $L_2$, and $L_3$ represent the soil layers of 0 cm–20 cm, 20 cm–40 cm, and 40 cm–60 cm under the cultivated land surface, respectively. The lowercase letters represent the significant difference in each soil layer's nutrient annual migration loss loads between different planting stages at $p = 0.05$. SD represents standard deviation. $S_1$ is the maize planting stage; $S_2$ is the summer fallow period; $S_3$ is the mustard planting stage; and $S_4$ is the winter fallow period.
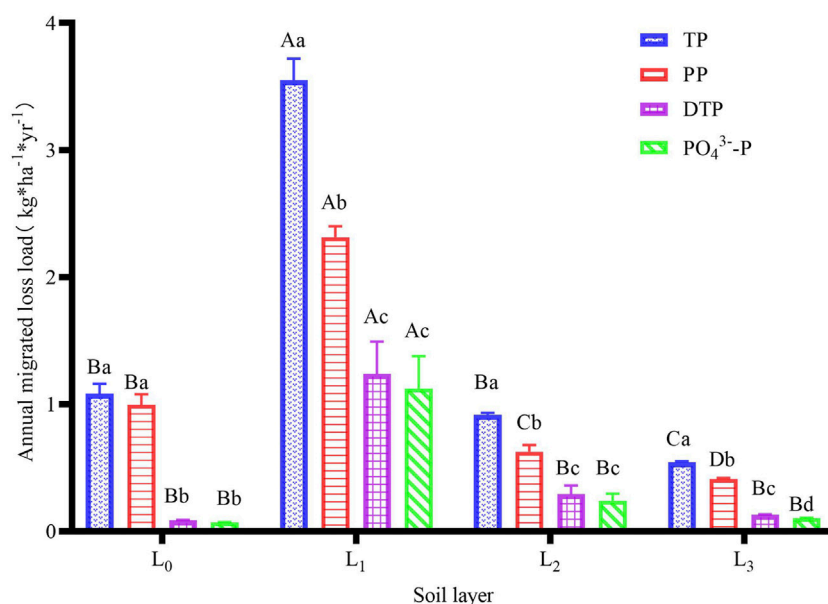
**FIGURE 6**
Annual migration loads of different P forms of each soil layer during the test period. TP, DTP, PP, and $PO_4^{3-}-P$ are the abbreviations of total phosphorus, total dissolved phosphorus, particulate phosphorus, and phosphate–phosphorus, respectively. The capital letters represent the significant difference between different soil layers at $p = 0.05$; the lowercase letters represent the significant difference between different P forms in the same soil layer at $p = 0.05$.
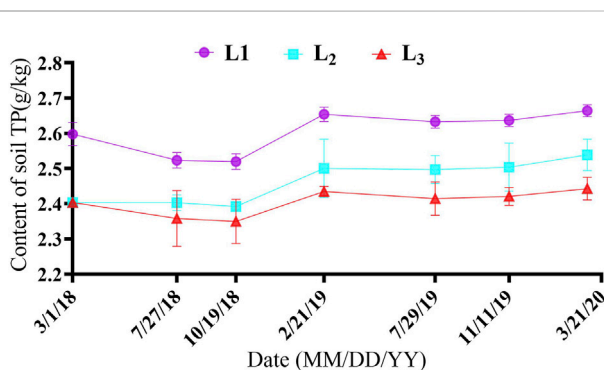


**FIGURE 7**
Change of each soil layer's TP content during the test period. $L_1$, $L_2$, and $L_3$ represent the soil layers of 0 cm–20 cm, 20 cm–40 cm, and 40 cm–60 cm under the cultivated land surface, respectively.

loads was 92.0%, similar to the proportion of 85%–94.1% obtained by Xie et al. (2014).

The bottom soil layers ($L_2$ and $L_3$) intercepted 84.7% of the underground lost P leached from the cultivated soil layer to enrich the subsoil P pool, similar to the result of more than 80% obtained by Gachter et al. (2004). This was mainly because the surface soil is rich in pores and cracks due to plant roots, soil microbial activity, and human activities. Under rainfall-runoff events, P leaches downward with water flow in pores or cracks (Kleinman et al., 2005) to transport topsoil P, especially PP, to the subsoil layers (Makowski et al., 2020). However, under gravity and leaching, after subsiding, the soil structure of the bottom layer is dense and has few soil pores

(Gachter et al., 2004; Peng et al., 2014). The bottom layer might hinder the migration process of sediment particles with adsorbed P. Wang et al. (2021a) found that the proportion of sediment particles 0.002 mm in size decreased significantly with an increase in the soil layer, which indirectly proved that the subsoil layers might affect the soil PP migration process. Gachter et al. (2004) found that the P content in the subsoil increased by 1.2–2.5 times after 15 years of fertilization and cultivation, further confirming that the subsoil layers had an interception and enrichment effect on the leaching of P from the soil. This result was also consistent with the research results obtained by Makowski et al. (2020), who reported that the underlying soil could intercept most sediment and particle nutrients lost from the cultivated soil layer. In this study, the soil TP of $L_1$, $L_2$, and $L_3$ improved by 2.57%, 5.61%, and 1.65%, respectively, after two consecutive years of monitoring in soil TP (Figure 7), which could prove the agricultural P migration rule in different soil layers. Moreover, Wang et al. (2022) concluded that annual P application led to greater accumulation of soil P in the topsoil layers in Northeast China. Therefore, P fertilizer should be applied to avoid P accumulation in the topsoil to limit P losses in surface runoff and leaching through the soil profile.

The large amount of applied fertilizer and the overlap with the rainstorm season cause the maize season to be the main period of P loss. In this study, it was found that soil P surface loss and underground leaching loss presented significant positive linear correlations with rainfall ($p < 0.05$), similar to the results obtained by McDowell et al. (2001). Heavy-rainfall events mostly occurred in the maize season and summer fallow period. In contrast, moderate and light rain was dominant, under which it was difficult to produce runoff in the mustard season. Simultaneous fertilization

and preferential flow channels are the major reasons for the sharp observed increases in P losses (Gachter et al., 1998; Stamm et al., 1998; Geohring et al., 2001; Barton et al., 2005). Therefore, the annual P loss load and proportion of PP were higher in the maize season and lower in the mustard season. Torrential and heavy rain events dominated the annual surface P loss, but heavy rain and moderate rain events controlled the annual underground P leaching load. The rainfall intensity and amount mostly controlled the surface P loss. The higher the rainfall intensity was, the greater the splash erosion degree, the faster the surface runoff yield, and the more PP loss occurred. However, soil P leaching was affected by the rainfall intensity and rainwater infiltration discharge. Heavy- and moderate-rain events could produce a certain amount of splashing sediment particles and ensure stable runoff production to ensure leached nutrient transport and carrying processes. This result was consistent with the work of Pu et al. (2014) and Zhang et al. (2016), who reported that higher rainfall could easily lead to increased loss of N and P in surface runoff. In conclusion, the prevention and control of P loss in purple soil sloping cultivated land should focus on preventing and controlling P loss in the cultivated soil layer during the maize and summer fallow seasons.

Remarkably, in this study, the soil layered filling and the installation of runoff troughs would damage the soil structure from top to bottom and increase the soil hydraulic conductivity, which might cause the soil phosphorus migration to be higher than the actual situation. Therefore, due to the aforementioned limitations of experimental conditions, the results of this experiment could not fully represent the soil P migration process in the natural sloping cropland of purple soil, but it could partially represent the soil P migration in the newly cultivated sloping farmland of purple soil in Chongqing.

## 5 Conclusion

The cultivated soil layer was the source of P loss on the purple soil sloping cropland. PP was the primary form of surface and subsurface P losses. Surface loss and underground leaching loss were two major loss pathways of P in the studied cultivated soil layer of purple soil sloping land under natural rainfall conditions. P's annual leaching loss from the cultivated soil layer was three times its surface loss. The bottom soil layers intercepted most of the P leached from the cultivated soil layer. Remarkably, 74.2% and 10.5% of the annual leached P were retained by the plow pan soil layer and parent material layer, respectively, to increase *in situ* soil P stocks. Only 15.3% of the annual leached P from the cultivated soil layer, almost half the annual surface P loss load, was eventually lost underground, and 43.9% of the annual surface P loss load was from the heavy-rain events on the purple soil sloping cropland during the test period. In comparison, 36.1%, 30.5%, and 30.3% of the annual leached loss underground were from heavy-, moderate-, and torrential-rain events, respectively. The maize season was the primary period of soil P surface and subsurface loss in hilly areas. Therefore, it is

important to strengthen the prevention and control of P migration losses in the maize season for surface losses and underground leached P losses. Furthermore, due to the limitations of experimental conditions, the results of this experiment could not fully represent the soil P migration process in the natural sloping cropland of purple soil, but it could partially represent the soil P migration in the newly cultivated sloping farmland of purple soil in Chongqing.

## Data availability statement

The raw data supporting the conclusion of this article will be made available by the authors, without undue reservation.

## Author contributions

Conceptualization and methodology: YW and JN; writing–original draft preparation: YW; writing–review and editing: FC and HZ; and project administration and funding acquisition: JN, DX, and DL. All authors contributed to the article and approved the submitted version.

## Funding

## Conflict of interest

The authors declare that the research was conducted in the absence of any commercial or financial relationships that could be construed as a potential conflict of interest.

## Publisher's note

All claims expressed in this article are solely those of the authors and do not necessarily represent those of their affiliated organizations, or those of the publisher, the editors, and the reviewers. Any product that may be evaluated in this article, or claim that may be made by its manufacturer, is not guaranteed or endorsed by the publisher.

## References

Bah, H. D., Zhou, M. H., Ren, X., Hu, L., Dong, Z. X., and Zhu, B. (2020). Effects of organic amendment applications on nitrogen and phosphorus losses from sloping cropland in the upper Yangtze River. *Agr. Ecosyst. Environ.* 302, 107086. doi:10.1016/j.agee.2020.107086

Barton, L., Schipper, L. A., Barkle, G. F., McLeod, M., Speir, T. W., Taylor, M. D., et al. (2005). Land application of domestic effluent onto four soil types: Plant uptake and nutrient leaching. *J. Environ. Qual.* 34 (2), 635–643. doi:10.2134/jeq2005.0635

Bechmann, M., Greipsland, I., and Ogaard, A. F. (2019). Implementation of mitigation measures to reduce phosphorus losses: The vestre vansjo pilot catchment. *Agriculture-Basel* 9 (1), 15–19. doi:10.3390/agriculture9010015

Cameron, K. C., Di, H. J., and Moir, J. L. (2013). Nitrogen losses from the soil/plant system: A review. *Ann. Appl. Biol.* 162 (2), 145–173. doi:10.1111/aab.12014

Chen, A., and Arai, Y. (2020). Current uncertainties in assessing the colloidal phosphorus loss from soil. *Adv. Agron.* 163, 117–151. doi:10.1016/bs.agron.2020.05.002

Cheng, Y. T., Li, P., Xu, G. C., Wang, X. K., Li, Z. B., Cheng, S. D., et al. (2021). Effects of dynamic factors of erosion on soil nitrogen and phosphorus loss under freeze-thaw conditions. *Geoderma* 390, 114972. doi:10.1016/j.geoderma.2021.114972

Deng, L. Z., Fei, K., Sun, T. Y., Zhang, L. P., Fan, X. J., Wu, Y. H., et al. (2020). Characteristics of phosphorus loss from the weathered granite slopes of Southeast China. *Pol. J. Environ. Stud.* 29 (3), 2139–2150. doi:10.15244/pjoes/111136

Fischer, P., Pothig, R., Gucker, B., and Venohr, M. (2018). Phosphorus saturation and superficial fertilizer application as key parameters to assess the risk of diffuse phosphorus losses from agricultural soils in Brazil. *Sci. Total Environ.* 630, 1515–1527. doi:10.1016/j.scitotenv.2018.02.070

Gachter, R., Ngatiah, J. M., and Stamm, C. (1998). Transport of phosphate from soil to surface waters by preferential flow. *Environ. Sci. Technol.* 32 (13), 1865–1869. doi:10.1021/es9707825

Gachter, R., Steingruber, S. M., Reinhardt, M., and Wehrli, B. (2004). Nutrient transfer from soil to surface waters: Differences between nitrate and phosphate. *Aquat. Sci.* 66 (1), 117–122. doi:10.1007/s00027-003-0661-x

Geohring, L. D., McHugh, O. V., Walter, M. T., Steenhuis, T. S., Akhtar, M. S., and Walter, M. F. (2001). Phosphorus transport into subsurface drains by macropores after manure applications: Implications for best manure management practices. *Soil Sci.* 166 (12), 896–909. doi:10.1097/00010694-200112000-00004

Hanrahan, B. R., King, K. W., Duncan, E. W., and Shedekar, V. S. (2021). Cover crops differentially influenced nitrogen and phosphorus loss in tile drainage and surface runoff from agricultural fields in Ohio, USA. *J. Environ. Manage* 293, 112910. doi:10.1016/j.jenvman.2021.112910

He, S., Li, F. Y., Liu, Z. W., Wang, Z. R., Wu, S. S., Zhang, T. Y., et al. (2019). Retarding effect of migration of colloidal phosphorus in three types of soil (in Chinese with English abstract). *J. Zhejiang Univ. (Agric. Life Sci.)* 45 (2), 205–210. doi:10.3785/j.issn.1008-9209.2018.03.262

Hua, K. K., and Zhu, B. (2020). Phosphorus loss through surface runoff and leaching in response to the long-term application of different organic amendments on sloping croplands. *J. Soil Sediment.* 20 (9), 3459–3471. doi:10.1007/s11368-020-02675-3

Huang, R., Gao, X. S., Wang, F. H., Xu, G. X., Long, Y., Wang, C. Q., et al. (2020). Effects of biochar incorporation and fertilizations on nitrogen and phosphorus losses through surface and subsurface flows in a sloping farmland of Entisol. *Agri Ecosyst. Environ.* 300, 106988. doi:10.1016/j.agee.2020.106988

Jahanzad, E., Saporito, L. S., Karsten, H. D., and Kleinman, P. J. A. (2019). Varying influence of dairy manure injection on phosphorus loss in runoff over four years. *J. Environ. Qual.* 48 (2), 450–458. doi:10.2134/jeq2018.05.0206

Kleinman, P. J. A., Srinivasan, M. S., Skarpley, A. N., and Gburek, W. J. (2005). Phosphorus leaching through intact soil columns before and after poultry manure application. *Soil Sci.* 170 (3), 153–166. doi:10.1097/00010694-200503000-00001

Li, Z. G., Gu, C. M., Zhang, R. H., Ibrahim, M., Zhang, G. S., Wang, L., et al. (2017). The benefic effect induced by biochar on soil erosion and nutrient loss of slopping land under natural rainfall conditions in central China. *Agr. Water Manage* 185, 145–150. doi:10.1016/j.agwat.2017.02.018

Linderholm, K., Mattsson, J. E., and Tillman, A. M. (2012). Phosphorus flows to and from Swedish agriculture and food chain. *Ambio* 41 (8), 883–893. doi:10.1007/s13280-012-0294-1

Liu, Y., Tao, Y., Wan, K. Y., Zhang, G. S., Liu, D. B., Xiong, G. Y., et al. (2012). Runoff and nutrient losses in citrus orchards on sloping land subjected to different surface mulching practices in the Danjiangkou Reservoir area of China. *Agr. Water Manage* 110, 34–40. doi:10.1016/j.agwat.2012.03.011

Luo, C., Gao, Y., Zhu, B., and Wang, T. (2013). Sprinkler-based rainfall simulation experiments to assess nitrogen and phosphorus losses from a hillslope cropland of purple soil in China. *Sustain Wat Quali Ecol* 1-2, 40–47. doi:10.1016/j.swaqe.2014.03.001

Makowski, V., Julich, S., Feger, K-H., and Julich, D. (2020). Soil phosphorus translocation via preferential flow pathways: A comparison of two sites with different phosphorus stocks. *Front Glob Chang* 3, 48. doi:10.3389/ffgc.2020.00048

McDowell, R., Sharpley, A., Brookes, P., and Poulton, P. (2001). Relationship between soil test phosphorus and phosphorus release to solution. *Soil Sci.* 166 (2), 137–149. doi:10.1097/00010694-200102000-00007

McDowell, R. W., Norris, M., and Cox, N. (2016). Using the provenance of sediment and bioavailable phosphorus to help mitigate water quality impact in an agricultural catchment. *J. Environ. Qual.* 45 (4), 1276–1285. doi:10.2134/jeq2015.10.0536

Ministry of Environmental Protection, and Mep, P. R. C. (2020). *Ecological and environmental monitoring of the yangtze three Gorges project bulletin 2018 2020-12-16*. Beijing: Ministry of Ecology and Environment of People's Republic of China. Available at: http://english.mee.gov.cn/Resources/Reports/.

Peng, X., Zhu, Q. H., Xie, Z. B., Darboux, F., and Holden, N. M. (2016). The impact of manure, straw and biochar amendments on aggregation and erosion in a hillslope Ultisol. *Catena* 138, 30–37. doi:10.1016/j.catena.2015.11.008

Peng, X. D., Shi, D. M., Jiang, D., Wang, S. S., and Li, Y. X. (2014). Runoff erosion process on different underlying surfaces from disturbed soils in the Three Gorges Reservoir Area, China. *Catena* 123, 215–224. doi:10.1016/j.catena.2014.08.012

Pisani, O., Liebert, D., Bosch, D. D., Coffin, A. W., Endale, D. M., Potter, T. L., et al. (2020). Element losses from fields in conventional and conservation tillage in the Atlantic Coastal Plain, Georgia, United States. *J. Soil Water Conserv.* 75 (3), 376–386. doi:10.2489/jswc.75.3.376

Plach, J. M., Macrae, M. L., Ali, G. A., Brunke, R. R., English, M. C., Ferguson, G., et al. (2018). Supply and transport limitations on phosphorus losses from agricultural fields in the lower great lakes region, Canada. *J. Environ. Qual.* 47 (1), 96–105. doi:10.2134/jeq2017.06.0234

Pu, Y. L., Xie, D. T., Lin, C. W., Ni, J. P., and Wei, C. F. (2014). Effect of hedgerow patterns controlling nitrogen loss of slope farmland in purple soil area (in Chinese with English abstract). *Trans. Chin. Soc. Agric. Eng.* 30 (23), 138–147. doi:10.3969/j.issn.1002-6819.2014.23.018

Stamm, C., Fluhler, H., Gachter, R., Leuenberger, J., and Wunderli, H. (1998). Preferential transport of phosphorus in drained grassland soils. *J. Environ. Qual.* 27 (3), 515–522. doi:10.2134/jeq1998.00472425002700030006x

Wang, M., Pendall, E., Fang, C. M., Li, B., and Nie, M. (2018). A global perspective on agroecosystem nitrogen cycles after returning crop residue. *Agr. Ecosyst. Environ.* 266, 49–54. doi:10.1016/j.agee.2018.07.019

Wang, Y., Ni, C. S., Wang, S., Xie, D., and Ni, J. P. (2021a). A reliable U-trough runoff collection method for quantifying the migration loads of nutrients at different soil layers under natural rainfall. *Sustainability* 13 (4), 2050. doi:10.3390/su13042050

Wang, Y., Ni, J. P., Ni, C. S., Wang, S., and Xie, D. T. (2021b). Effect of natural rainfall on the migration characteristics of runoff and sediment on purple soil sloping cropland during different planting stages. *J. Water Clim. Change* 12 (7), 3064–3081. doi:10.2166/wcc.2021.333

Wang, Y. (2021). "Research on N and P loss load and nutrient balance under farming-mulberry system on purple soil sloping cropland of Three Gorge Reservoir Area,". Thesis: Ph. D. in *Chinese with English abstract* (Chongqing, China: Southwest University).

Wang, Y. Z., Peng, X. Y., Whalen, J. K., Shi, Y., Lu, C. Y., Huang, B., et al. (2022). Can periodic phosphorus fertilizer applications reduce the risk of P loss. *Nutr. Cycl. Agroecosys* 124, 135–151. doi:10.1007/s10705-021-10184-z

Weihrauch, C., and Weber, C. J. (2021). Comparative risk assessment of phosphorus loss from "deep phosphorus stocks" in floodplain subsoils to surface waters. *Sci. Total Environ.* 796, 149037. doi:10.1016/j.scitotenv.2021.149037

Xie, D. T., Ni, J. P., Ding, E. J., and al, e. (2014). *Study on control technology of agricultural non-point source pollution in Three Gorges reservoir area (in Chinese)*. Beijing: Science Press. ISBN: 978-7-03-042100-5.

Yang, J. H., Wang, C. L., and Dai, H. L. (2008). *Soil agrochemical analysis and environmental monitoring*. Beijing: China Land Press. In Chinese.

Zhang, T., Ni, J. P., and Xie, D. T. (2015). Severe situation of rural non-point source pollution and efficient utilization of agricultural wastes in the Three Gorges Reservoir Area. *Environ. Sci. Pollut. R.* 22 (21), 16453–16462. doi:10.1007/s11356-015-5429-z

Zhang, Y., Fan, F. L., Zhou, C., Ni, J. P., and Xie, D. T. (2016). Effects of crop/mulberry intercropping on surface nitrogen and phosphorus losses in Three Gorges Reservoir Area (in Chinese with English abstract). *Acta Pedol. Sin.* 53 (1), 189–201. doi:10.11766/trxb201507160248

Zhang, Y., Xie, D. T., Ni, J. P., and Zeng, X. B. (2019). Optimizing phosphate fertilizer application to reduce nutrient loss in a mustard (Brassica juncea var. tumida)-maize (Zea mays L) rotation system in Three Gorges Reservoir area. *Soil Till Res.* 190, 78–85. doi:10.1016/j.still.2019.03.001

Zhang, Z. Y., Kong, L. L., Zhu, L., and Mwiya, R. M. (2013). Effect of drainage ditch layout on nitrogen loss by runoff from an agricultural watershed. *Pedosphere* 23 (2), 256–264. doi:10.1016/s1002-0160(13)60014-4

Zhu, B., Wang, Z. H., Wang, T., and Dong, Z. X. (2012). Non-Point-source nitrogen and phosphorus loadings from a small watershed in the three Gorges Reservoir area. *J. Mt. Sci-Engl.* 9 (1), 10–15. doi:10.1007/s11629-012-2196-x

Zuo, F. L., Li, X. Y., Yang, X. F., Wang, Y., Ma, Y. J., Huang, Y. H., et al. (2020). Soil particle-size distribution and aggregate stability of new reconstructed purple soil affected by soil erosion in overland flow. *J. Soil Sediment.* 20 (1), 272–283. doi:10.1007/s11368-019-02408-1